



Effect of cooling rate on transformation temperature measurements of $Ti_{50}Ni_{50}$ alloy by differential scanning calorimetry and dynamic mechanical analysis

S.H. Chang, S.K. Wu*

Department of Materials Science and Engineering, National Taiwan University, Taipei 106, Taiwan

ARTICLE DATA

Article history:

Received 19 July 2007

Accepted 7 August 2007

Keywords:

Shape memory alloy

Martensitic transformation

Differential scanning calorimetry (DSC)

Dynamic mechanical analysis (DMA)

Cooling rate effect

ABSTRACT

Martensitic transformation temperatures of a $Ti_{50}Ni_{50}$ shape memory alloy measured by both differential scanning calorimetry and dynamic mechanical analysis decrease with increased cooling rate. The transformation temperature determined by differential scanning calorimetry, with greater mass, increases more rapidly at slower cooling rates but this specimen size effect becomes negligible when the cooling rate is close to zero. The cooling rate effect is more significant with dynamic mechanical analysis than with differential scanning calorimetry due to the larger specimen/furnace sizes used for the former, which results in a greater temperature gradient.

© 2007 Elsevier Inc. All rights reserved.

1. Introduction

TiNi-based alloys are among the most important shape memory alloys (SMAs) because of their excellent shape memory effect (SME) and superelasticity [1]. Many studies have revealed that TiNi-based SMAs also exhibit a high internal friction peak associated with a shear modulus minimum during martensitic transformation, and are thus suitable for energy dissipation applications [2–13]. It has been reported that the damping characteristics of internal friction peak(s) in TiNi-based SMAs are closely related to experimental parameters such as temperature cooling/heating rate \dot{T} , frequency ν , and applied stress amplitude σ_0 [2,4]. A dynamic mechanical analyzer (DMA) is an instrument of absolute accuracy and repeatability, which can measure the $\tan \delta$ and storage modulus E_0 of the specimen by applying a sinusoidal amplitude σ_0 with a given ν and \dot{T} [14]. Therefore, DMA is suitable for studying the damping characteristics of internal friction peak(s) in TiNi SMAs by controlling accurately the

experimental parameters [15–19]. Chang and Wu [17–19] have investigated the inherent internal friction of $Ti_{50}Ni_{50}$ SMA during martensitic transformation by DMA and noticed that there is always a temperature shift between the martensitic transformation peak(s) measured at a constant \dot{T} and those measured under isothermal treatment. This phenomenon implies that the martensitic transformation temperature measured by DMA is apparently affected by the cooling/heating rate. It has also been reported that the martensitic transformation temperature is influenced by the cooling/heating rate used in differential scanning calorimetry (DSC) tests [20,21], but this effect has not yet been systematically investigated. In this study, martensitic transformation temperatures of $Ti_{50}Ni_{50}$ SMA were measured by DSC and DMA with various cooling rates \dot{T} . Thereafter, the cooling rate effect on the martensitic transformation temperatures measured by DSC and DMA is discussed. At the same time, the differences in the cooling rate effect on transformation temperatures determined by DSC and DMA tests are compared.

* Corresponding author. Tel.: +886 2 2363 7846; fax: +886 2 2363 4562.
E-mail address: skw@ntu.edu.tw (S.K. Wu).

2. Experimental Procedures

Ti₅₀Ni₅₀ SMA was prepared by conventional vacuum arc remelting. The as-melted ingot was hot-rolled at 850 °C into a 2-mm-thick plate and then solution-treated at 850 °C for 2 h followed by quenching in water. Subsequently, the hot-rolled and solution-treated plate was cut into test specimens with dimensions of 42.5×9.7×1.5 mm (weight about 4066 mg) for DMA tests and with masses of 9.8 mg, 24.5 mg and 132.4 mg for DSC tests. Transformation temperatures and tan δ values of the hot-rolled and solution-treated Ti₅₀Ni₅₀ specimens were measured by TA 2980 DMA equipment with different cooling rate \dot{T} from 0.5 °C/min to 5 °C/min. Values of ν and σ_0 used were 1 Hz and 5 μ m, respectively. Transformation temperatures of the hot-rolled and solution-treated Ti₅₀Ni₅₀ specimens were also determined by DSC tests, using TA Q10 DSC equipment with different sample masses and various \dot{T} from 3 °C/min to 40 °C/min. The maxima \dot{T} used in the DMA and DSC tests were chosen as 5 °C/min and 40 °C/min, respectively, because a \dot{T} value higher than 5 °C/min for DMA or 40 °C/min for DSC can exceed the capacity of the respective liquid nitrogen cooling systems. On the other hand, the minima \dot{T} used in DMA and DSC tests were chosen as 0.5 °C/min and

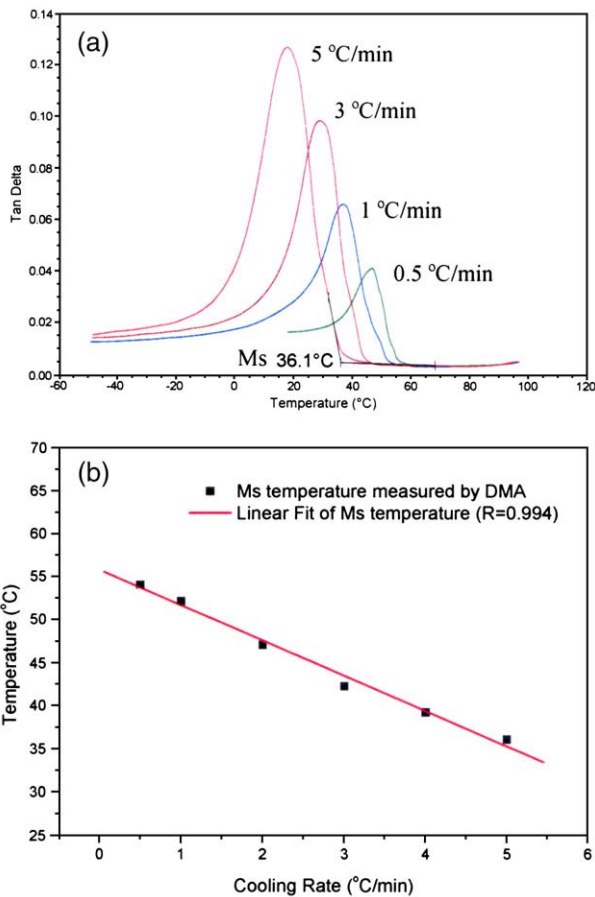


Fig. 1 – (a) DMA results of Ti₅₀Ni₅₀ specimens measured at different cooling rates. (b) The measured Ms temperatures from (a) as a function of cooling rate.

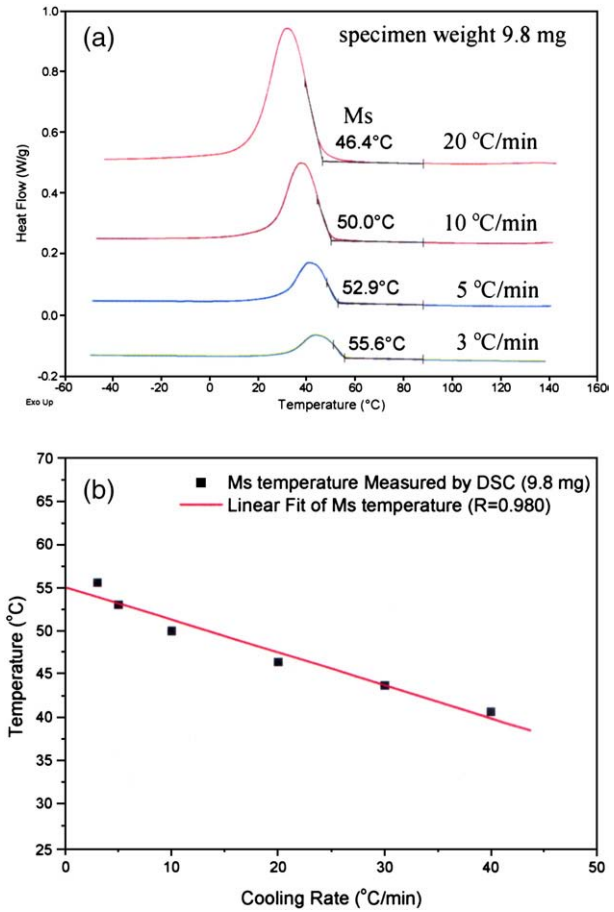


Fig. 2 – (a) DSC results of Ti₅₀Ni₅₀ specimens measured at different cooling rates. (b) The measured Ms temperatures from (a) as a function of cooling rate. The weight of the specimen was 9.8 mg.

3 °C/min, respectively, because the transformation peak becomes inconspicuous when a \dot{T} value is too low.

3. Results and Discussion

3.1. Cooling Rate Effect on DMA and DSC Measurements

Fig. 1(a) shows the tan δ curves of Ti₅₀Ni₅₀ specimens measured by DMA at cooling rates from 0.5 °C/min to 5 °C/min. As shown in Fig. 1(a), we also represent schematically how to determine the martensite starting temperature (Ms temperature) from the cooling tan δ curve. Fig. 1(b) plots the Ms temperatures measured from Fig. 1(a) as a function of \dot{T} . As shown in Fig. 1(a), the tan δ values of the transformation peaks decrease with decreasing \dot{T} . This characteristic has been demonstrated by the Dejonghe–Delorme model [2] in which the magnitude of the tan δ value is a function of \dot{T} . Moreover, as illustrated in Fig. 1(b), the Ms temperatures measured by DMA increase linearly with decreasing \dot{T} . Fig. 2(a) shows the cooling curves for 9.8 mg Ti₅₀Ni₅₀ specimens measured by DSC at various cooling rates \dot{T} . Fig. 2(b) plots the Ms temperatures measured from Fig. 2(a) as a function of \dot{T} . As can be seen in Fig. 2(b), the Ms temperatures measured by DSC also increase

with decreasing \dot{T} . This phenomenon indicates that the \dot{T} effect on martensitic transformation temperatures is similar in DSC and DMA tests.

3.2. Specimen Weight Effect on DSC Measurement Under Different Cooling Rates

In order to investigate the specimen weight effect on the martensitic transformation temperature, the transformation behavior of hot-rolled and solution-treated $Ti_{50}Ni_{50}$ specimens with different specimen weights were determined by DSC at cooling rates \dot{T} ranging from 3 °C/min to 40 °C/min; Fig. 3 presents the results. As seen in Fig. 3, the Ms temperatures of each weight-group of specimens increased with decreasing \dot{T} . Also, the Ms temperatures of the heaviest specimens increased more rapidly with decreasing \dot{T} . This reflects the fact that the larger specimen size leads to a greater temperature gradient from the center to the surface of the specimen when it is cooled or heated at a constant rate. Therefore, the cooling rate effect on the Ms temperatures is more significant when a heavier specimen is used in DSC measurement. Note also that all the curve-fitting lines for the Ms temperatures vs. \dot{T} measured by DSC are close to 55 °C when \dot{T} approaches zero. This feature indicates that the specimen weight effect on the Ms temperature by DSC measurement becomes negligible when \dot{T} is close to zero.

3.3. The Discrepancy of Martensitic Ttransformation Temperatures Measured by DMA and DSC

Fig. 4 plots the measured Ms temperatures vs. \dot{T} presented in Figs. 1(b) and 2(b). As shown in Fig. 4, with increasing \dot{T} the Ms temperatures measured by DMA decline faster than those measured by DSC. This indicates that the cooling rate effect on martensitic transformation temperatures in DMA test is more significant than that in DSC tests; this is explained by the different specimen and furnace (load-cell) sizes inherently designed into the DSC and DMA instruments.

In Fig. 4, the size and mass of the DMA specimens are 42.5 × 9.7 × 1.5 mm and 4066 mg, respectively, while those of DSC

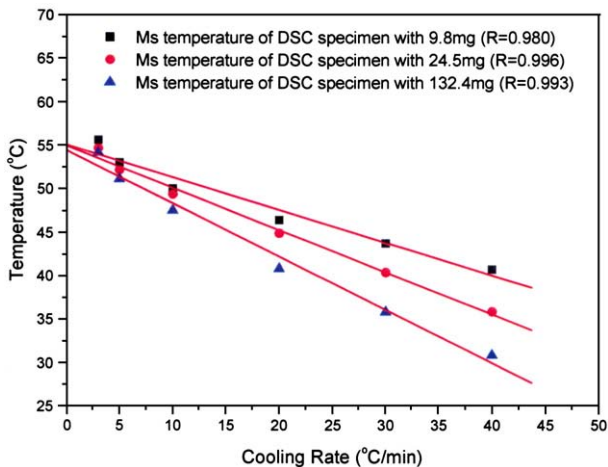


Fig. 3 – The Ms temperatures of $Ti_{50}Ni_{50}$ specimens with different sizes measured by DSC as a function of cooling rate.

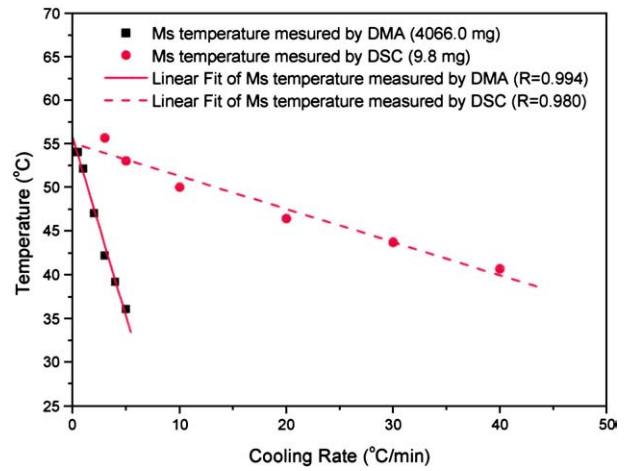


Fig. 4 – The Ms temperatures of $Ti_{50}Ni_{50}$ specimens measured by DMA and DSC as a function of cooling rate. The weight of the DSC specimen was 9.8 mg.

specimens are only 1.3 × 1.0 × 1.5 mm and 9.8 mg, respectively. In other words, the mass of the DMA specimens is about 400 times greater than that of the DSC specimens. Therefore, according to the specimen weight effect discussed previously, the \dot{T} effect on the Ms temperature in DMA tests should be more significant than in DSC tests. In addition, the DSC specimen is sealed in an aluminum pan during testing while the DMA specimen is directly loaded onto a single cantilever clamp. Consequently, it can be expected that the complex heat fluxes in the DMA furnace resulting from the heater, purge gas and liquid nitrogen cause a larger temperature gradient in the DMA specimen. In addition, the furnace size of the DMA equipment (TA 2980 DMA) is much larger than that of the DSC equipment (TA Q10 DSC). The larger furnace size creates a greater temperature gradient between the heater and thermocouple and provides a bigger thermal resistance when the specimen is heated or cooled at a constant rate. Hence, the \dot{T} effect is more significant and causes higher decreasing rates of the Ms temperatures vs. \dot{T} in DMA measurements. However, as illustrated in Fig. 4, the curve fitting lines of the Ms temperatures vs. \dot{T} measured by DSC and DMA eventually approach the same value (about 55 °C) when \dot{T} approaches zero. This phenomenon reveals that differences in the \dot{T} effect on the Ms temperatures between DSC and DMA tests can be negligible when the cooling rate approaches zero. Hence, the observed \dot{T} effect on the measured Ms temperatures can be considered as merely a technical problem due to the different specimen and furnace sizes inherently to the DSC and DMA instruments.

4. Conclusions

The effect of cooling rate \dot{T} on martensitic transformation temperatures of $Ti_{50}Ni_{50}$ SMA measured by DSC and DMA tests was investigated in this study. Experimental results reveal that martensitic transformation temperatures measured by both DSC and DMA increase with decreasing \dot{T} . The much greater mass of specimens used for DMA tests cause a much more rapid decrease in the measured Ms temperatures with decreasing \dot{T} . This reflects the greater temperature gradient from the center to

the surface of the specimen when it is cooled or heated at a constant rate. Differences in the results measured by either technique become insignificant when the cooling rate \dot{T} approaches zero. At cooling rates near zero, the Ms temperatures measured by either technique approach 55 °C.

Acknowledgment

The authors gratefully acknowledge the financial support for this research provided by the National Science Council (NSC), Taiwan, Republic of China, under Grant No. NSC95-2221-E002-164.

REFERENCES

- [1] Wayman CM, Durning TW. In: Durning TW, Melton KN, Stöckel D, Wayman CM, editors. *Engineering aspects of shape memory alloys*. London: Butterworth-Heinemann; 1990.
- [2] Dejonghe W, Debatist R, Delaey L. Factors affecting internal-friction peak due to thermoelastic martensitic-transformation. *Scr Metall* 1976;10:1125–8.
- [3] Sugimoto K, Mori T, Otsuka K, Shimizu K. Simultaneous measurements of internal-friction, Young's modulus and shape change associated with thermoelastic martensite-transformation in Cu–Al–Ni single-crystals. *Scr Metall* 1974;8:1341–8.
- [4] Mercier O, Melton KN, De Prévaille Y. Low-frequency internal-friction peaks associated with the martensitic phase-transformation of NiTi. *Acta Metall* 1979;27:1467–75.
- [5] Iwasaki K, Hasiguti R. Effect of preannealings on the temperature spectra of internal-friction and shear modulus of Ti–51Ni. *Trans JIM* 1987;28:363–7.
- [6] Wu SK, Lin HC, Chou TS. A study of electrical-resistivity, internal-friction and shear modulus on an aged Ti₄₉Ni₅₁ alloy. *Acta Metall* 1990;38:95–102.
- [7] Liu Y, Van Humbeeck J, Stalmans R, Delaey L. Some aspects of the properties of NiTi shape memory alloy. *J Alloys Compd* 1997;247:115–21.
- [8] Coluzzi B, Biscarini A, Campanella R, Trotta L, Mazzolai G, Tuissi A, et al. Mechanical spectroscopy and twin boundary properties in a Ni_{50.8}Ti_{49.2} alloy. *Acta Mater* 1999;47:1965–76.
- [9] Biscarini A, Campanella R, Coluzzi B, Mazzolai G, Trotta L, Tuissi A, et al. Martensitic transitions and mechanical spectroscopy of Ni_{50.8}Ti_{49.2} alloy containing hydrogen. *Acta Mater* 1999;47:4525–33.
- [10] Coluzzi B, Biscarini A, Campanella R, Mazzolai G, Trotta L, Mazzolai FM. Effect of thermal cycling through the martensitic transition on the internal friction and Young's modulus of a Ni_{50.8}Ti_{49.2} alloy. *J Alloys Compd* 2000;310:300–5.
- [11] Mazzolai FM, Biscarini A, Campanella R, Coluzzi B, Mazzolai G, Rotini A, et al. Internal friction spectra of the Ni₄₀Ti₅₀Cu₁₀ shape memory alloy charged with hydrogen. *Acta Mater* 2003;51:573–83.
- [12] Yoshida I, Monma D, Iino K, Ono T, Otsuka K, Asai M. Internal friction of Ti–Ni–Cu ternary shape memory alloys. *Mater Sci Eng A Struct Mater Prop Microstruct Process* 2004;370:444–8.
- [13] Mazzolai FM, Coluzzi B, Mazzolai G, Biscarini A. Hydrogen diffusion and interpretation of the 200 K anelastic relaxation in NiTi alloys. *Appl Phys Lett* 2004;85:2756–8.
- [14] Menard KP. *Dynamic mechanical analysis: a practical introduction*. Boca Raton: CRC Press; 1999.
- [15] Chang SH, Wu SK. Textures in cold-rolled and annealed Ti₅₀Ni₅₀ shape memory alloy. *Scr Mater* 2004;50:937–41.
- [16] Chang SH, Wu SK. Damping characteristics of cold-rolled and annealed equiatomic TiNi shape memory alloy. *Key Eng Mater* 2006;319:9–15.
- [17] Chang SH, Wu SK. Inherent internal friction of B2? R and R? B19' martensitic transformations in equiatomic TiNi shape memory alloy. *Scr Mater* 2006;55:311–4.
- [18] Chang SH, Wu SK. Internal friction of R-phase and B19' martensite in equiatomic TiNi shape memory alloy under isothermal conditions. *J Alloys Compd* 2007;437:120–6.
- [19] Chang SH, Wu SK. Internal friction of B2 → B19' martensitic transformation of Ti₅₀Ni₅₀ shape memory alloy under isothermal conditions. *Mater Sci Eng A Struct Mater Prop Microstruct Process* 2007;454–455:379–83.
- [20] Shield TW. Orientation dependence of the pseudoelastic behavior of single-crystals of Cu–Al–Ni in tension. *J Mech Phys Solids* 1995;43:869–95.
- [21] An L, Huang WM. Transformation characteristics of shape memory alloys in a thermal cycle. *Mater Sci Eng A Struct Mater Prop Microstruct Process* 2006;420:220–7.